Topographic Distribution of UnCovered Areas (UCA) in Full Tone Flexographic Prints

Gustavo Gil Barros; Carl-Magnus Fahlcrantz & Per-Åke Johansson*

Keywords: Flexography, Topography, Printability, UCA

Abstract: Local unprinted areas of a full-tone printed substrate, UCA (uncovered areas), occur when incomplete ink transfer takes place during the printing process. This paper proposes a method for characterizing the substrate topography in the uncovered areas in a flexographic print. Fourteen graphic boards, printed using an IGT-F1 laboratory press, were analyzed with an integrated instrument consisting of the STFI grazing light topography characterization method (OptiTopo) and an UCA detection algorithm. The validity of the algorithm was verified by visual evaluation. The analysis of frequency distribution of UCA occurrence suggests a strong link between UCA occurrence and the topographic character of the substrate. A close inspection decisively indicates that surface depressions are the driving cause of uncovered areas. Frequency analysis and two different models of topographic thresholding were successfully tested as predictors of UCA occurrence.

Introduction

Flexography is currently one of the fastest growing printing processes, both in volume and in market share. Higher quality and improved runnability, combined with the relative simplicity and low costs of the process, are the driving forces for the present expansion.

Research in the field was initially aimed at identifying the main factors influencing the printing mechanism. The relative importance and interactions between the identified factors are now being studied in an effort to establish functional models describing the flexographic process. Once an accurate general model is available, the ability to predict attainable print quality may become a reality to the benefit of both the paper and the printing industries.

Previous work (Aspler, 1998) (Jewell, 2000) showed that ink transfer is directly influenced by substrate and print forme properties in combination with factors such as pressure and speed. Surface roughness and the hardness of the forme were shown to be more important than the surface energy when considering attainable print quality (Lindholm, 1998) (Lavelle, 1996). Substrate properties

*STFI-Packforsk AB, Box 5604, 114 86 Stockholm, Sweden

such as roughness and absorbancy are recognized to play a dominant role for printability, whereas substrate surface chemistry appears to have less influence (Sheng, 2000) (Lagerstedt, 1997) (Zang, 1995). The importance of paper topography for flexographic printability is generally well accepted.
Local unprinted areas in a full-tone print due to incomplete ink transfer, so-called "uncovered areas", are serious blemishes compromising print quality. This work attempts to clarify the relation between the occurrence of uncovered areas and the topographic characteristics of the print substrate. Integrating a surface topography characterization method (OptiTopo) with an UCA detection algorithm has made it possible to separately characterize the topographical features of the uncovered areas.

Theory

OptiTopo is a contactless, optically based 3-D scanning instrument developed at the Swedish Pulp and Paper Research Institute (STFI). It makes it possible to obtain precise and fast topographic images from both printed and unprinted paper surfaces. The detection principle is based on a new photometric stereo theory successfully introduced for paper evaluation during 1999 (Hansson, 1999). Using CCD video acquisition equipment, two images of the same area of a paper surface are acquired, illuminated respectively by grazing light in opposite directions. By assuming a model for the light scattering properties of the paper surface and measuring the variation between the shadows and highlights produced by a fully characterized grazing light source, it is possible to compute the slopes composing such a surface. In this way a partial derivative of the surface height is obtained and these data are then integrated to generate a topographic 3D image. In the case of a printed sample, and because the method is based on standard digital video, both initial images can be combined using proper compensation for the low lighting angles and an intensity image can be generated equivalent to if the surface were illuminated under homogeneous light (i.e. as an observer would perceive the printed motive under normal observation conditions). The applied photometric stereo theory also verifies that, when the scanned sample is printed using transparent ink (i.e. the majority of process colors), the gradient obtained and the calculated topography remain largely unaffected by the presence of the ink layer. The simultaneous extraction of two independent pictures from the same surface area, carrying respectively the topography and the reflectance information, is therefore possible. The OptiTopo principle and its application to the characterization of paper substrates has been previously demonstrated by Hansson (2000). Additional advantages of the technique are its easiness of use and speed (total acquisition and calculation time does not exceed 5 seconds), the variable range of scanned areas and its applicability to a wide variety of paper grades.

Ink-covered regions of a full-tone print generally have reflectance values that are relatively low compared to the reflectance value of a white substrate. Uncovered

or non-printed regions in the image can thus be detected by finding the areas presenting reflectance values higher than a certain threshold value. Let such a threshold, *TR*, define a reflectance level that separates image areas considered to be covered with ink from areas that are considered to be uncovered:

$$TR = R_{med} + 0.20 * WPD \quad (1)$$

where R_{med} is the median of the image reflectance values and *WPD* (White Point Distance) is the distance, in reflectance units, between the White Point and the median of the image reflectance values, R_{med}. The White Point is a theoretical concept corresponding to a reflectance of 100%, an absolute quantity representing a perfectly white substrate. Applying the obtained threshold value, *TR*, to a reflectance-calibrated image allows the creation of a binary mask that spatially highlights uncovered areas and separates them from ink-covered ones. The integration of the proposed UCA detection algorithm into the previously described OptiTopo technique makes it possible to separately characterize the topographical distribution of the uncovered areas of a printed sample and to study the impact of the substrate surface topography on the ink transfer process.

In its initial development form, the OptiTopo technique does not provide a reflectance-calibrated intensity image, as required for the application of the UCA detection algorithm. The images are acquired in gray levels using a 12 bits dynamic range, which is kept during the calculation process. The attainable quality is therefore dependent on the general performance of the video camera, the linearity of its response and the choice of settings employed for the acquisition (e.g. diaphragm opening and digital shutter speed). In order to obtain an accurate reflectance-calibrated intensity image of a printed surface, two major improvements were introduced to the algorithm: 1) a different compensation for the light distribution inhomogeneity and 2) a reflectance calibration. The combination of both upgrades provides a generally more stable and homogeneous response.

As previously stated, the intensity image results from the combination of two images of the same surface illuminated by low angle light of opposite directions. In order to avoid any artificially induced gradients in the intensity image, a light distribution correction is applied to each of the primary images. Gradients can be caused by a small geometric misalignment of the lamp orientation. The same correction also compensates for the fact that the illumination is provided by standard dichroic spotlights instead of ideal parallel lighting as required by the general theory. The new compensation is based on a standard 3D background correction of the spotlight-induced gradient, modeled by a polynomial least-mean-squares approximation of the light distribution shape (Russ, 1999). Tests where the new correction model was applied to a topographically flat reference sample with a homogeneous reflectance level showed a decrease in the coefficient of variation of the resulting intensity image from 2.5% to 1.3%, as

evidence of the method's efficiency. The new method made it possible to generate an intensity image virtually free of patterns, gradients or perturbations. Such a homogeneous image can have its gray level information converted to reflectance, thereby compensating for any possible asymmetry in the light sources' emitted intensity and simultaneously providing a linear scale of representation.

Several tests conducted using reference gray patches from the NCS series (Natural Color System from the Scandinavian Colour Institute) made it possible to characterize the response of the CCD camera and determine its linear working range. The reflectances of the reference patches were associated to the colorimetric Y values measured using a Gretag SPM 100-II spectrophotometer. The choice of measuring instrument was mainly determined by the similar geometries of the Gretag spectrophotometer and the OptiTopo, associated with the possibility of measuring using a polarizing filter. A stable and linear correspondence between the camera's gray level and the reflectance value of the sample made it possible to define a conversion relation based on a simple slope. The slope parameters only require two points to be fully described, and they can be calculated using two fully characterized reference samples, thus creating a two-point calibration. A stability study of the CCD camera showed a stable black level (i.e. average gray level corresponding to the mean intensity of the camera noise), which made it possible to reduce the calibration requirement to a single point, by replacing one point with the black level. In this way, only one reference standard patch is required each time any OptiTopo setting is changed, in order to calculate the correct conversion slope. Accuracy tests, performed using the most common OptiTopo configurations, indicated a maximum total error less than two units of Y when such a calibration model was used.

Method

Printing Trials

Printing Press. The samples were printed using an IGT-F1 laboratory flexo press equipped with a copper engraved anilox roll, reference 402.208 (4.5 ml/m^2 - 45° - 140 l/cm) at a speed of 0.6m/s using two inking revolutions of the impression cylinder before printing (flexo multiple revolutions mode). The printing forme was a solid (full-tone) photopolymer with a thickness of 1.7mm, 50mm width, hardness 55 Shore A and a surface energy of 38.0mN/m (measurement technique: see *substrates*). It was assembled using a 0.54mm thick Lohmann mounting tape creating a final cylinder with a diameter of 170.45mm, in agreement with the manufacture specifications (IGT Systems, 2002). In order to maximize the amount of uncovered area induced, the printing force was set to 50N corresponding to the lowest feasible operational level (i.e. limit before slip occurs). The anilox force was set to 35N following a recommendation that the ratio of the anilox to the printing force be as close as

possible to ⅔. The trials were carried out in a standard conditioned room (23°C; 50% RH).

Ink. A water-based cyan ink, Scanbrite Raster B60750 from Sun Chemicals was used. The ink was adjusted to 23s DIN Cup #4 using demineralised water, corresponding to a final viscosity of 180cP measured with a Brookfield viscometer RVDV-I (spindle N° 2; measuring speed 100rpm) and had a surface tension of 32.9mN/m measured using the DuNouy ring method.

Substrates. A total of 14 commercial boards covering a wide range of roughness levels and different applications were printed. The resulting print densities were measured by a Gretag SPM 100-II spectrophotometer using C illuminant, 10º observer with polarizing filter. The samples' surface energies were estimated following the Owens & Wendt approach using dematerialized water and diiodomethane (DIM). The contact angles were measured at 0.1s after drop release (assuming this time to be sufficient for drop stabilization) using a DAT 1100 - Dynamic Contact Angle instrument from FIBRO system AB - Sweden. The indicated spreading power corresponds to the difference between the sample surface energy and the ink surface tension in mN/m. The main properties of the substrates are summarized in Table 1.

Table 1: *Properties of the printed substrates. Note that the extremely fast absorption of the diiodomethane by the Calendared Board sample meant its surface energy could not be estimated by the present method.*

Samples	Grammage [g/m^2]	PPS10 [µm]	Surface Energy [mN/m]	Spreading Power [mN/m]	Print Density
White Liner	274	2	39.7	6.8	2.64
Full Coated Board	136	2.03	43.5	10.6	2.57
White Top Kraft	197	2.1	40.7	7.8	2.58
Light Coated Board	130	2.26	42.2	9.3	2.39
Calendared Board	160	4.45	-	-	1.68
White Liner	298	5.0	35.3	2.4	2.08
Bleached Board	140	6.08	37.0	4.1	1.69
White Top Kraft Liner 1	140	6.71	44.5	11.6	1.56
White Top Test Liner 1	140	6.76	38.4	5.5	1.40
White Top Kraft Liner 2	142	7.08	41.8	8.9	1.56
White Top Kraft Liner 3	142	7.61	44.3	11.4	1.34
Semi Bleached Kraft	140	8.19	38.9	6.0	1.17
White Top Test Liner 2	140	9.55	38.4	5.5	1.04
White Top Test Liner 3	140	9.78	39.2	6.3	0.76

Visual Assessment of UCA

Samples. A suitable area of 40x40mm^2 was selected from the second half of each printed strip according to the IGT recommendations. The 14 samples were then mounted onto white opaque propylene plates (0.8mm) using double-sided tape (0.02mm) for stability and protection before any evaluation took place.

Observers. A panel of 10 observers, 4 male and 6 female, with an experience in the assessment of print-induced non-quality artifacts ranging from nothing to extensive, was enrolled. All observers had normal or corrected-to-normal vision.

Procedure. The evaluation was conducted in a perception laboratory with a homogeneous overhead light source (1400lx, 5000K). The observers were asked to estimate the amount of uncovered area in each of the 14 prints, i.e. to state what percentage of the total area of the prints they considered not to be covered with ink.

Instrumental Evaluation

OptiTopo Acquisition & Processing. Four independent areas of 16x16mm^2 on each sample were scanned by the OptiTopo instrument with a resolution of 31.25μm per pixel. The new improved version of the instrument was employed to obtain the reflectance-calibrated intensity, the uncovered area detection binary mask and the topography image from each of the scanned areas.

Topography & UCA. The binary detection mask obtained by the UCA detection algorithm was first applied to calculate a general indicator of the UCA amount. This measure is calculated as a percentage of the total area considered not to be covered with ink.

Combining the UCA detection binary mask with a bandpassed (wavelength 0.01-0.5mm) topographic image of the same surface, it was possible to extract the topography information of the substrate portion not covered with ink (i.e. where UCA occurs). Considering the instrument's working resolution (31.25μm) and the chosen bandpass range, the filter acts solely as a low pass. The general resilience of the printing forme system together with the printing nip contact dimensions determine the appropriate choice of long-wave cut-off. This choice was made in order to filter out long-wave components from the paper surface whose influence on the final result is minimized by the press action during printing. For each scanned area, the total topography histogram as well as the histogram of its uncovered regions were calculated using the same class distribution (-20μm to 20μm with 0.25μm steps). Because the same classes are used, a direct division of both histograms generates a new histogram displaying the UCA occurrence frequency distribution. This measure makes it

possible to statistically estimate the probability of UCA occurrence at each substrate height level. See example in Figure 1.

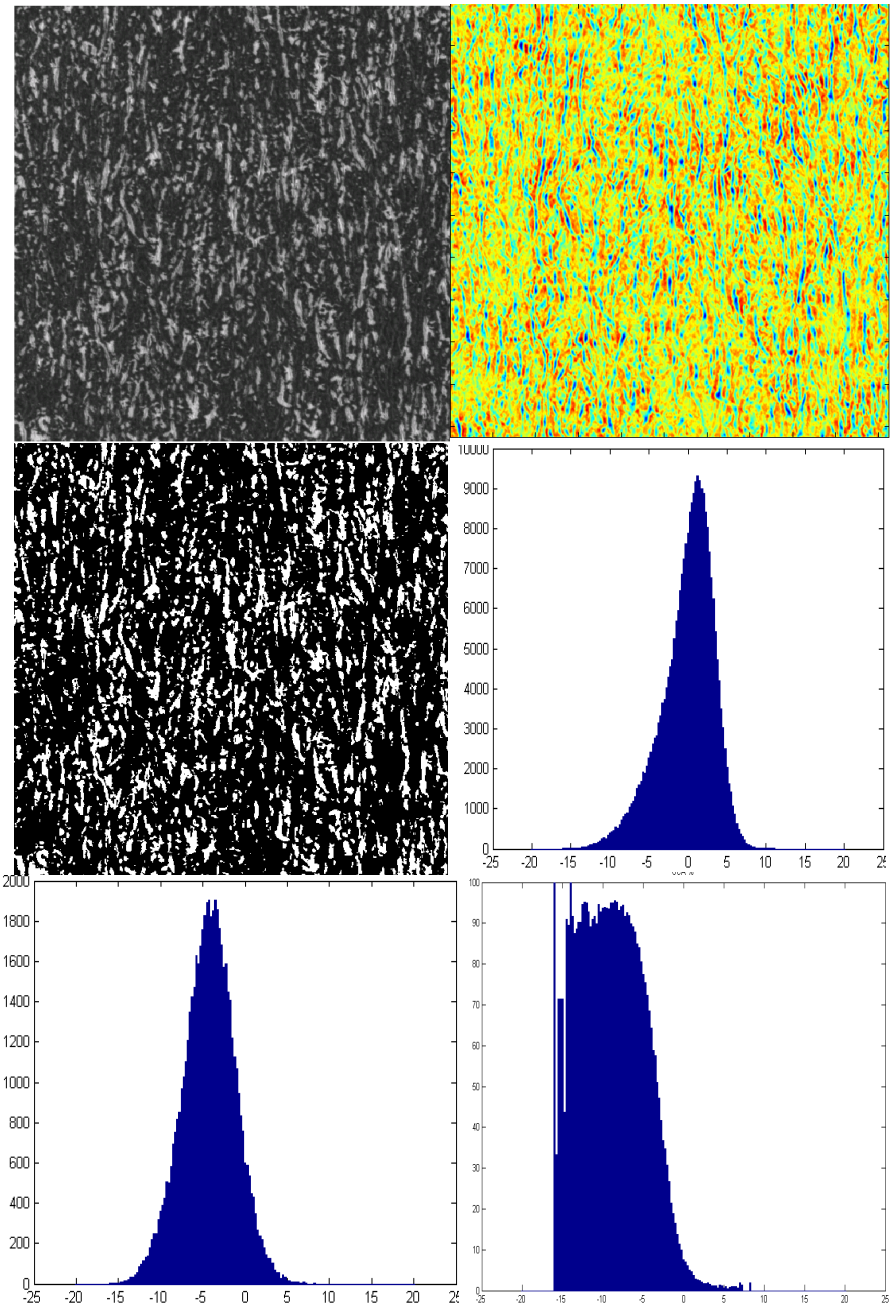

Figure 1: *Application of the UCA detection algorithm and subsequent calculation of the frequency distribution of the UCA topography for a rough board (example White Top Test Liner 3 with approximately 22% UCA). From left to right: reflectance-calibrated intensity, bandpassed topography, UCA binary detection mask, total topography histogram, height histogram of the uncovered areas and UCA occurrence frequency distribution.*

Results

Visual assessment of the UCA detection algorithm

The agreement between observers was 0.95, calculated as the arithmetic mean of the Fisher's z transformed inter-individual Pearson correlation coefficients (Fisher, 1924). The correspondence between visual assessment and instrumental detection of UCA is presented in Figure 2. The relationship is however far from being linear, as is evident in the left-hand diagram. The linearized model presented in a log:log diagram to the right in Figure 2 yielded a coefficient of determination of 0.96.

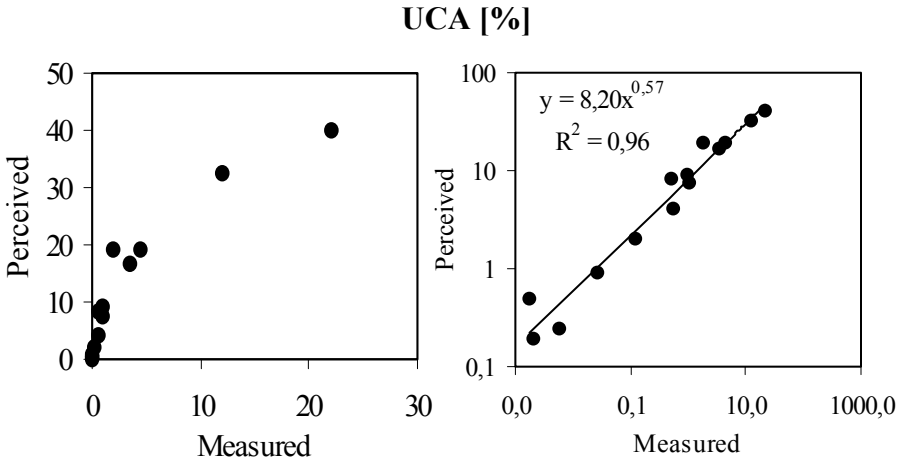

Figure 2: *Visual assessment versus instrumental detection of UCA, with a linear scale on the left and a log:log scale on the right.*

Topographic characteristics of uncovered areas

Histograms reflecting the UCA occurrence frequency distribution according to the topography were calculated for each sample, combining the four scanned areas of each sample into a single large area. A representability limit was established with a minimum of ten occurrences per height class (classes with fewer counts were not considered), which limits the practical applicability of the process to samples having a certain minimum quantity of UCA. Figure 3 displays some of the UCA occurrence frequency distributions according to topography. The general shape shows that the frequency of UCA occurrence sharply raises for deeper pits (negative height).

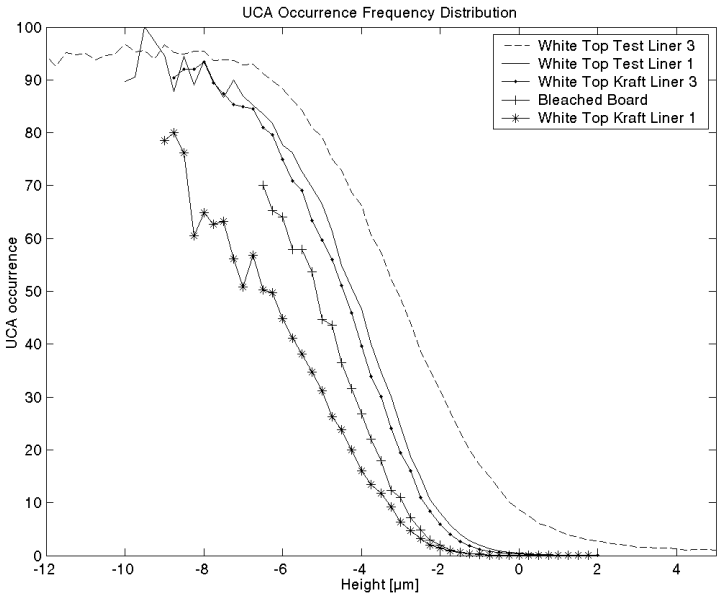

Figure 3: *UCA occurrence frequency distribution according to topography for various samples.*

UCA predictability using topography spectral analysis

A spectral analysis of the substrate topography was performed to investigate the possibility of establishing a statistical prediction model. Table 2 contains the topography's variance distributed per octave wavelength band for each sample. The correlation between the variance in each octave band and the UCA occurrence indicated that 0.125-0.25mm, 0.25-0.5mm and 0.5-1mm are the most suitable passbands for use as a predictor. Figure 4 displays the relation between the UCA value and the printed substrate roughness (measured as the 0.25-0.5mm bandpassed variance). The simple linear predictor model shown has a coefficient of determination of 0.92.

Table 2: *Spectral analysis of the substrate topography calculated as variance per octave band, UCA value and correlation between UCA and each octave band.*

	Variance [μm^2] per wavelength [mm]							UCA
Sample	0.0625-0.125	0.125-0.25	0.25-0.5	0.5-1	1-2	2-4	4-8	[%]
White Liner	0.01	0.03	0.05	0.08	0.35	0.99	3.10	0.01
Full Coated Board	0.02	0.08	0.13	0.21	0.41	1.01	1.46	0.00
White Top Kraft	0.01	0.04	0.06	0.09	0.49	1.61	6.16	0.12
Light Coated Board	0.02	0.07	0.11	0.24	0.59	1.38	1.93	0.00
Calendared Board	0.03	0.10	0.23	0.55	1.29	2.79	8.95	0.03
White Liner	0.01	0.09	0.21	0.52	1.16	1.91	4.63	0.55
Bleached Board	0.04	0.23	0.49	0.75	1.31	1.76	5.11	0.53
White Top Kraft Liner 1	0.08	0.53	1.15	1.98	2.28	2.78	5.43	0.98
White Top Test Liner 1	0.11	0.70	1.50	1.87	1.78	2.06	3.80	4.44
White Top Kraft Liner 2	0.05	0.28	0.64	1.29	2.10	2.79	5.60	1.01
White Top Kraft Liner 3	0.10	0.73	1.41	1.55	1.66	1.75	3.19	3.48
Semi Bleached Kraft	0.09	0.92	2.36	2.71	2.64	2.40	3.93	1.88
White Top Test Liner 2	0.10	0.82	2.96	5.15	5.92	10.10	15.71	12.01
White Top Test Liner 3	0.17	2.51	7.88	8.36	5.37	3.66	5.40	21.99
Correlation Coefficient	0.81	0.92	0.96	0.97	0.87	0.57	0.38	

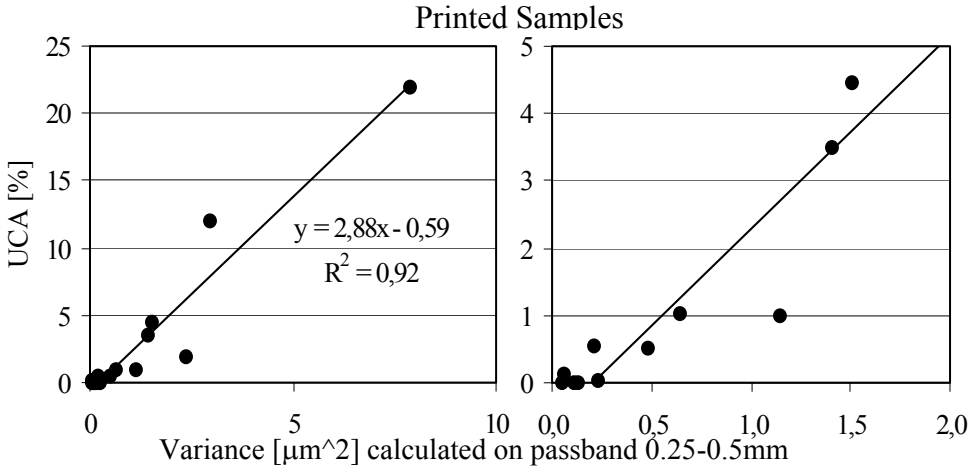

Figure 4: *Relation between the UCA value and substrate roughness in the passband* 0.25-0.5mm*, predictability based on a linear approximation. Left and right figures: full range and enlarged high quality range.*

UCA predictability by topography thresholding

The feasibility of a prediction model based on topography thresholding was studied by plotting the UCA value against the total surface area below a defined height threshold in a bandpassed topographic image (same bandwidth as for the UCA algorithm, 0.01-0.5mm). This deterministic model assumes the existence of a critical depth (negative height level) greater than which no ink transfer can occur. Therefore the proportion of the surface area corresponding to this criterion is considered to be a prediction of UCA. Figure 5 (upper) contains the suggested plot for different depth thresholds for all samples. A magnified version of the data between 0% and 5% is displayed in Figure 5 (lower). Each point corresponds to a different sample and is the average of four independently scanned areas. Both graphs contain a reference 1:1 line, which marks the location of a perfect correspondence between predicted and measured UCA.
An attempt was made to choose an appropriate UCA predictor using a constant threshold. The best correlation was obtained for a threshold of -4µm, with a correlation coefficient of 0.97. This is a high degree of correlation, although the UCA percentage predicted with this threshold is smaller than that actually measured by the detection algorithm.

An alternative predictor was tested in which a variable threshold was used in order to obtain a direct estimation of the measured UCA. A relationship was graphically obtained from Figure 5, by determining for each UCA level what would be the optimal choice of height threshold, *Vtr – variable threshold*, required for such a predictor:

$$Vtr = -3.5 + 0.06 * UCA \quad (2)$$

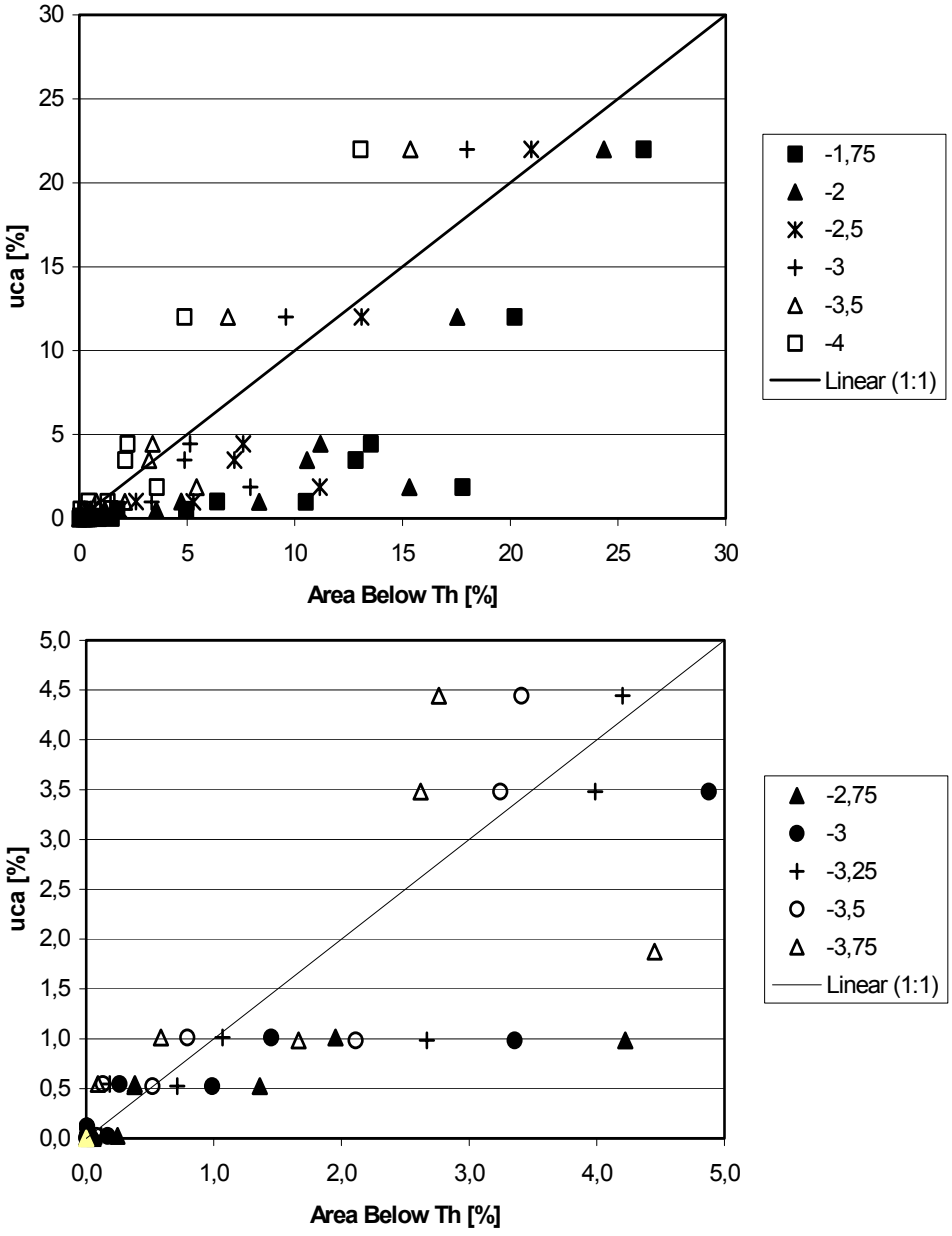

Figure 5: *Relation between the measured UCA and the total surface area below different height thresholds on the bandpassed (0.01-0.5mm) height images of each sample. Upper and lower figures: full range and enlarged high quality range.*

Table 3 is a compilation of the results obtained when both predictors are applied to the complete set of samples. The table also includes results obtained using the classical Parker Print-Surf air-leak device (PPS10) for comparison purposes. The data are graphically represented in figure 6 and 7.

Table 3:*UCA prediction results for all samples using both constant and dynamic models.*

			Prediction Models		
			Constant	Variable	
Samples	PPS10	UCA [%]	Area [%]	Tr [μm]	Area [%]
White Liner	2	0.01	0.00	-3.50	0.00
Full Coated Board	2.03	0.00	0.00	-3.50	0.00
White Top Kraft	2.1	0.12	0.00	-3.49	0.00
Light Coated Board	2.26	0.00	0.01	-3.50	0.01
Calendared Board	4.45	0.03	0.04	-3.50	0.08
White Liner	5	0.55	0.07	-3.47	0.14
Bleached Board	6.08	0.53	0.27	-3.47	0.54
White Top Kraft Liner 1	6.71	0.98	1.31	-3.44	2.24
White Top Test Liner 1	6.76	4.44	2.23	-3.23	4.27
White Top Kraft Liner 2	7.08	1.01	0.43	-3.44	0.86
White Top Kraft Liner 3	7.61	3.48	2.13	-3.29	3.86
Semi Bleached Kraft	8.19	1.88	3.60	-3.39	5.95
White Top Test Liner 2	9.55	12.01	4.88	-2.78	11.03
White Top Test Liner 3	9.78	21.99	13.05	-2.18	23.08
Correlation Coefficient	0.93*		0.97		0.98
Determination Coeff.	0.86*		0.93		0.96

* Using an exponential model.

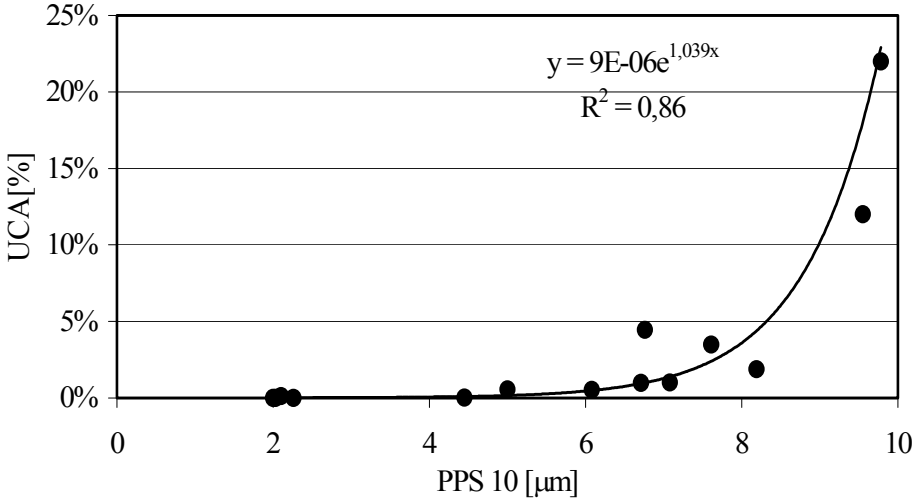

Figure 6: *UCA versus PPS10 roughness*

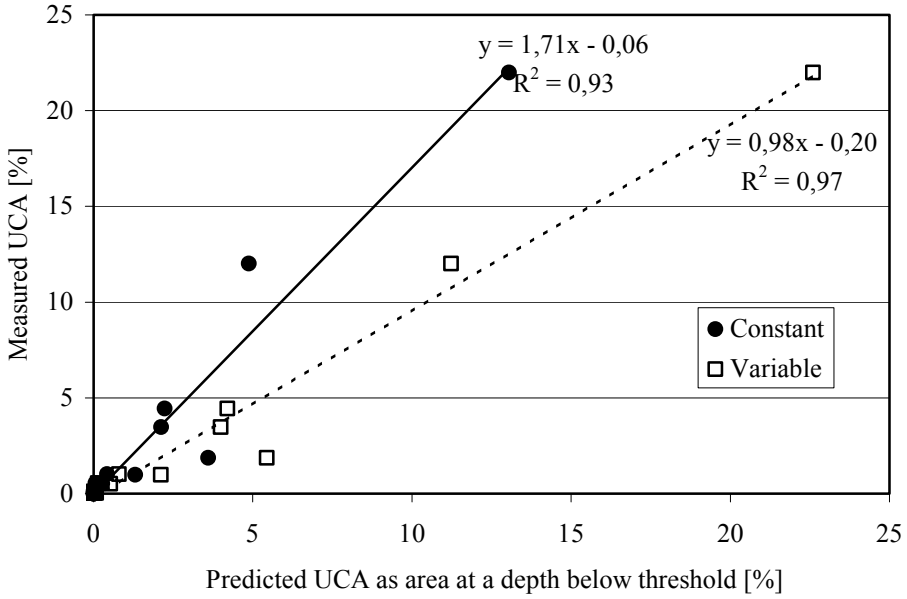

Figure 7: *Applicability and precision of two proposed predictors based on topographic thresholds: constant (-4µm) and variable (Vtr).*

Discussion

The introduction of a reflectance calibration into OptiTopo proved to be viable but it gave a limited accuracy, the maximum error has been estimated to two Y units. The present result is a compromise between quality and usability. Disrupting this equilibrium by using a larger number of calibration points would improve the accuracy at the expense of user friendliness. To reproduce using a CCD camera the results measured by a colorimeter has proven to be difficult, mainly due to the dissimilarity of the principles employed. However, taking into account the non-optimal illumination used (i.e. type of light combined with demanding geometry), the accuracy and stability of the reflectance transformation was found to be suitable for UCA detection.

The UCA detection algorithm was successfully validated by the high correlation with the visual assessment of the printed samples (Figure 2). The general performance of the detection algorithm, judged in relation to human perception, could perhaps be enhanced if the calculation were based on CIELAB lightness (L*) values instead of the luminous reflectance factor (Y). The lightness value takes better account of the non-linearity of the human visual system. The white point concept used as a reference starting point for the UCA calculation assumes that the substrate is white, and this works well for papers with high reflectance levels, due to the nature of human perception of luminance. However with extremely non-white samples (e.g. brownish unbleached Kraft pulp) this assumption is less valid. The misjudgment of the Semi-Bleached Kraft sample, visible in Figure 2 (left) as an outsider, illustrates this. The effect of using the white point concept could be minimized by substituting it with the reflectance value of the unprinted substrate. As in the case of a densitometric measurement, the paper white would then be an input to the system. Such an approach would improve the system's sensitivity but it would require the availability of a non-printed sample and reduce the user friendliness by increasing the number of operations.

The samples used in this study were a selection of commercial grades, mainly packaging boards and graphic liners, covering a wide range of roughness levels as shown by their PPS10 values (Table 3). They were printed using a laboratory device (IGT-F1) that only partially reproduces the conditions of a real press, particularly with regard to print speed and ink metering principle. Nevertheless this device is one of the few commercially available options for printing under fully controlled conditions, particularly with respect to the applied pressures. The multivariate origin of uncovered area induced during flexographic printing includes the print forme character, printing pressure, substrate and ink properties.
Printing forme hardness influences the mechanical contact between ink film and paper surface, since a softer forme deforms more easily under pressure. Forme resilience affects the dynamics of the deformation, and is thus important in high-

speed printing. The combined influence of both forme properties together with those of the mounting tape determines the degree of mechanical compliance between polymer and substrate surfaces. In order to confirm that no UCA was induced due to surface energy incompatibilities, the forme wettability was checked using a measure of ink spreading power. Using the multi-revolutions mode of the IGT-F1 a good homogenization of the ink on the forme surface was ensured, creating a uniform ink film which minimizes the risk that UCA could be induced by the ink metering system.
The choice of print pressure is crucial for the creation of UCA. At higher pressure levels, less UCA occurs but quality losses due to mechanical dot gain and mottle become important. The flexographic process rests on the kiss-print principle, where little pressure is applied, giving an optimized trade-off between the non-quality risks. In the present work, a low and constant printing pressure level was chosen.
Different substrates are expected to have very different properties regarding bulk, compressibility, roughness and surface energy. Bulk and particularly compressibility play a major role under increasing nip pressure, but since print pressure was very low their influence was not considered. The surface energy of the samples was studied and the spreading power of the ink was calculated in order to determine their relative affinities. All samples proved wettable and no direct link between UCA and spreading power could be established. Nevertheless the possibility that the surface energy may have a higher order effect should not be ignored. Absorbency, pre-wetting and drop instability due to roughness are recognized sources of inaccuracy when the contact angle method is used, so that is mainly an indicative measure. Substrate roughness has been the main focus of this study.
Different paper grades (e.g. coated or uncoated) will in practice be printed under very different conditions, reflecting different degrees of demand and expected quality. It would thus be legitimate to adjust the print settings to match the substrate type in order to reflect the print shop reality. A constant print setting was however used in order to facilitate a full comparison between grades and to test the applicability of a general printability hypothesis.

A simple mechanistic and deterministic description of the ink transfer in a flexographic nip based purely on substrate topography provides an explanation of UCA incidence and ink distribution in general. Assuming a non-deformable, non-compressible and wettable surface, the transfer of ink can be explained simply by the occurrence of contact during printing. In such a simplified representation, deep depressions on the surface (pits), where no contact with ink is possible, are the driving cause of UCA. On the other hand, peaks in the surface structure can under nip constraints lead to an increase in the local pressure and can cause the liquid ink to flow away from such locations and thus induce UCA or at least a locally thinner ink layer. In reality, substrates are deformable, compressible, absorbent and highly inhomogeneous in their composition, which adds a certain degree of randomness to the model. The

general dynamics of the printing process variables need be fully considered if an even more complete description is to be given.
The findings based on the frequency distribution of UCA occurrence support to a great extent this theory. The incidence of UCA was measured in probabilistic terms as a function of substrate height for different samples. The similarity of the shapes of the different distributions confirm the predominant role of topographic depressions for the non-transfer mechanism.

Besides providing a general understanding of the phenomena, the main goal of establishing a model is to permit predictions and forecasts. A spectral analysis of the topography provided an accurate estimator of UCA magnitude, but it is a general statistical predictor and is therefore not capable of providing information regarding the location of the occurrence. Its high degree of explanation corroborates previous findings regarding topography and UCA. In addition, the fact that the variance is analogous to the square of the height deviations reinforces the notion that extreme values (deep pits) are the driving cause of UCA.
The Parker Print-Surf instrument is an air-leak device commonly used for the estimation of surface roughness. The PPS results show a good correlation with the attainable print density (R=0.98) and give a general indication of the UCA magnitude but the relationship is not linear and the prediction power is limited (see Figure 6), i.e. samples having similar PPS10 values do not necessarily exhibit the same proportion of UCA. One explanation may lie in the difference in magnitude of the applied forces, the pressure applied by the PPS clamp is clearly higher than the flexo printing pressure.
The results obtained with thresholding predictors support the hypothesis of a contact-driven UCA directly influenced by the substrate roughness. Two major differences separate the two methods: correctness of UCA prediction and ease of application. The constant threshold method is directly applicable to the topographic map of an unprinted surface but the predicted UCA percentage tends to be too low, especially on rougher surfaces. On the other hand, the variable thresholding method gives predictions which closely correspond to the UCA measured on printed samples, but the method requires a knowledge of the UCA range to be studied. On an unprinted sample, it can only be applied in an iterative mode, where a constant threshold measurement gives a first UCA estimate which can be used to generate a new adapted threshold. In any case the choice of threshold must be adjusted to the actual printing process to be modelled since parameters such as ink film thickness and contact pressure directly influence the demands for a flawless print. An accurate UCA prediction in both magnitude and location will most probably also require other parameters than mere height values. The present models could be improved by introducing a wider notion of pit properties, where other geometric parameters such as radius, slope, spatial distribution and frequency of occurrence of pits are taken into account.

Conclusions

An optical technique for characterization of paperboard surfaces has been investigated and refined for the purpose of estimating the risk of non-ink covered areas, so called UCA, in flexo printing. The integration of a UCA detection algorithm made it possible to confirm that UCA is in fact associated with depressions in the surface topography. The method gives a fast recording of the surface topography and reveals sites of pits that are probably too deep to promote ink transfer. Results suggest that UCA estimations obtained in this way or through a variance analysis of the topography are superior to those based on traditional surface roughness measurements (e.g. the PPS air-leak instrument). The method should therefore be seen as a useful tool in the development of high quality print surfaces.

Acknowledgements

The financial support for this work from the Surface Treatment Programme at Karlstad University, Sweden is grateful acknowledge.
The authors would also like to express their gratitude to: Anders From of SCA Packaging R&D, Sundsvall, Sweden, for providing paper samples; Astrid Glasenapp and Behudin Mešić for assistance with test print advice and materials; Miroslav Hoc for help with surface energy measurements; Jan-Erik Nordström for valuable suggestions and discussions; all of whom are at STFI-Packforsk AB, Stockholm, Sweden.

References

Aspler, J. S., Jordan, B., Zang, Y. H., and Nguyen, N.
1998 "Print quality of linerboard in commercial water based flexography," Paper presented at TAGA 50th annual technical conference,

Fisher, R. A.
1924 "On a Distribution Yielding the Error Functions of Several Well Known Statistics," Paper presented at International Congress of Mathematics, Toronto,

Hansson, P., and Johansson, P. A.
1999 "A new method for the simultaneous measurement of surface topography and ink distribution on prints," Nord Pulp Pap Res J, vol. 14, no. 4, pp. 314-319.

Hansson, P., and Johansson, P. A.
2000 "Topography and reflectance analysis of paper surfaces using a photometric stereo method," Optical Engineering, vol. 39, no. 9, pp. 2555-2561.

IGT Systems,
2002 "IGT-F1 Printability Tester User Manual", IGT Testing Systems b.v., Amsterdam

Jewell, E. H., Claypole, T. C., Bohan, M. F. J., and Von Grol, M.

2000 "Modelling the flow in a flexographic ink chamber," Paper presented at TAGA 52nd annual technical conference, Pike's Peak, Colorado Springs, USA, Apr. 2000.

Lagerstedt, P., Kolseth, P., and Nordstrom, J. E. P.

1997 "Influence of surface energetics on ink transfer in flexo printing," Advances in printing science and technology 23: proceedings of the 23rd research conference of IARIGAI, Chichester, UK, 17-20 Sept. 1995.

Lavelle, J. S., Quinn, J. A., Gallagher, J. E., and Micale, F. J.

1996 "Measurement of flexographic ink transfer on a modified Prufbau," Paper presented at 1996 International printing and graphic arts conference, Atlanta, GA, USA, 16-19 Sept. 1996.

Lindholm, G.

1998 "Ink transfer in flexo," Flexo, vol. 23, no. 2, pp. 40-45.

Russ, J. C.

1999 "The image processing handbook" (CRC Press, Boca Raton, Florida), Third ed., 771pp.

Sheng, Y. J., Shen, W., and Parker, I. H.

2000 "The importance of the substrate surface energetics in water-based flexographic printing," Appita, vol. 53, no. 5, pp. 367-370.

Zang, Y. H., and Aspler, J. S.

1995 "Factors That Affect the Flexographic Printability of Linerboards," Tappi J, vol. 78, no. 10, pp. 240-23-240-33.